Journal of Catalysis **181,** 233–243 (1999)
Article ID jcat.1998.2305, available online at http://www.idealibrary.com on IDEAL®

Oxidation of SO_2 over Supported Metal Oxide Catalysts

Joseph P. Dunn,[1] Harvey G. Stenger, Jr., and Israel E. Wachs[2]

Zettlemoyer Center for Surface Studies, Department of Chemical Engineering, Lehigh University, Bethlehem, Pennsylvania 18015

Received June 19, 1998; revised October 10, 1998; accepted October 19, 1998

A systematic catalytic investigation of the sulfur dioxide oxidation reactivity of several binary (M_xO_y/TiO_2) and ternary ($V_2O_5/M_xO_y/TiO_2$) supported metal oxide catalysts was conducted. Raman spectroscopy characterization of the supported metal oxide catalysts revealed that the metal oxide components were essentially 100% dispersed as surface metal oxide species. Isolated fourfold coordinated metal oxide surface species are present for most oxides tested at low coverages, whereas at surface coverages approaching monolayer polymerized surface metal oxide species with sixfold coordination are present for some of the oxides. The sulfur dioxide oxidation turnover frequencies (SO_2 molecules converted per surface redox site per second) of the binary catalysts were all within an order of magnitude ($V_2O_5/TiO_2 > Fe_2O_3/TiO_2 > Re_2O_7/TiO_2 \sim CrO_3/TiO_2 \sim Nb_2O_5/TiO_2 > MoO_3/TiO_2 \sim WO_3/TiO_2$). An exception was the K_2O/TiO_2 catalyst system, which is inactive for sulfur dioxide oxidation under the chosen reaction conditions. With the exception of K_2O, all of the surface metal oxide species present in the ternary catalysts (i.e., oxides of V, Fe, Re, Cr, Nb, Mo, and W) can undergo redox cycles and oxidize sulfur dioxide to sulfur trioxide. The turnover frequency for SO_2 oxidation over all of these catalysts is approximately the same at both low and high surface coverages, despite structural differences in the surface metal oxide overlayers. This indicates that the mechanism of sulfur dioxide oxidation is not sensitive to the coordination of the surface metal oxide species. A comparison of the activities of the ternary catalysts with the corresponding binary catalysts suggests that the surface vanadium oxide and the additive surface oxide redox sites act independently without synergistic interactions: the sum of the individual activities of the binary catalysts quantitatively correspond to the activity of the corresponding ternary catalyst. The $V_2O_5/K_2O/TiO_2$ catalyst showed a dramatic reduction in catalytic activity in comparison to the unpromoted V_2O_5/TiO_2 catalyst. The ability of potassium oxide to significantly retard the redox potential of the surface vanadia species is primarily responsible for the lower catalytic reactivity.

Key Words: **sulfur dioxide; sulfur trioxide; oxidation; metal oxide; SCR; Raman; catalyst.**

INTRODUCTION

Sulfur dioxide (SO_2) is formed from both the oxidation of sulfur contained in fossil fuels and the industrial processes that treat and produce sulfur-containing compounds. The catalytic oxidation of sulfur dioxide appears in numerous industrial processes and has a significant environmental impact because of the associated sulfur oxide (SO_x) emissions. Approximately two-thirds of the 50 billion pounds of sulfur oxides released annually in the United States are emitted from coal fired power plants. Industrial fuel combustion and industrial processes (primarily sulfuric acid manufacture, petroleum refining, and smelting of nonferrous metals) account for the remainder of the emissions (1).

The oxidation of sulfur dioxide to sulfur trioxide is undesirable during the selective catalytic reduction (SCR) of nitrogen oxides (NO_x) found in the flue gas of power plants. SCR removes NO_x in the flue gas by reacting the nitrogen oxides with ammonia and oxygen to form nitrogen and water at approximately 370°C over titania supported vanadia catalysts, e.g., $V_2O_5/WO_3–MoO_3/TiO_2$ (2). Under typical SCR design and operating conditions, NO_x reduction efficiency is directly proportional to the $NH_3:NO_x$ ratio up to NO_x reduction levels of about 80%. Ammonia readily combines with sulfur trioxide at temperatures below 250°C to form ammonium sulfates, which can block the catalyst's pores and foul downstream heat exchangers. This problem is so serious that industrial specifications for SCR processes include upper limits for the outlet concentration of sulfur trioxide corresponding to approximately 1 to 2% sulfur dioxide conversion. Commercial SCR catalysts traditionally have low vanadia loadings due to vanadia's propensity to catalyze sulfur dioxide oxidation. Additives that can efficiently promote the SCR reaction without significantly increasing the rate of SO_2 oxidation would allow lower SCR operating temperatures without the worry of ammonium sulfate production and deposition.

In an effort to develop a catalyst for the selective catalytic reduction of nitric oxide with ammonia with minimal sulfur dioxide oxidation activity, Morikawa *et al.* (3) tested several modifications of vanadia/titania catalysts for sulfur dioxide oxidation and SCR activity (e.g., $V_2O_5/M_xO_y/TiO_2$, where $M_xO_y = GeO_2$, ZnO, MoO_3, or WO_3). Catalysts containing

[1] Current address: BOC Gases Technology, 100 Mountain Avenue, Murray Hill, NJ 07974.

[2] To whom correspondence should be addressed. Fax: (610) 758-6555. E-mail: iew0@lehigh.edu.

0021-9517/99 $30.00

tungsten oxide or molybdenum trioxide showed an increase in the activity of sulfur dioxide oxidation, while catalysts containing germanium oxide or zinc oxide showed a drastic decrease in sulfur dioxide oxidation activity. Similarly, Sazonova *et al.* (4) tested the performance of V_2O_5/TiO_2 catalysts doped by tungsten oxide and niobium oxide for sulfur dioxide oxidation and selective catalytic reduction of nitric oxide by ammonia. In contrast to the results of Morikawa *et al.*, the data suggest that tungsten oxide substantially decreases the oxidation of sulfur dioxide to sulfur trioxide. Niobium doped catalysts also exhibited a slight decrease in oxidation activity. Neither of these studies provided molecular structural information on the surface arrangement of the catalysts and, consequently, a fundamental explanation of the observed results could not be provided.

The objective of this investigation is to combine molecular structural information on several binary (e.g., V_2O_5/TiO_2, Re_2O_7/TiO_2, CrO_3/TiO_2, Fe_2O_3/TiO_2, Nb_2O_5/TiO_2, MoO_3/TiO_2, WO_3/TiO_2, and K_2O/TiO_2) and ternary (e.g., $V_2O_5/Re_2O_7/TiO_2$, $V_2O_5/CrO_3/TiO_2$, $V_2O_5/Fe_2O_3/TiO_2$, $V_2O_5/Nb_2O_5/TiO_2$, $V_2O_5/MoO_3/TiO_2$, $V_2O_5/WO_3/TiO_2$, and $V_2O_5/K_2O/TiO_2$) supported metal oxide catalysts with the corresponding sulfur dioxide oxidation reactivities in order to assist in the molecular engineering of SCR catalysts with low sulfur dioxide oxidation activities. This study does not investigate the abilities of these catalysts to efficiently promote the SCR of NO_x with NH_3, since a recent comprehensive study by Amiridis *et al.* (5) has addressed this issue.

METHODS

Preparation of Catalysts

The oxidation catalysts used in this research program were supported metal oxide catalysts possessing two-dimensional metal oxide overlayers on a high surface area titanium dioxide support. The two-dimensional metal oxide overlayers are confirmed by Raman spectroscopy and presented under Results. As shown in Table 1, the kinetic studies employed both low surface coverage (0.1 to 0.2 monolayer) and high surface coverage (0.7 to 0.9 monolayer) of supported vanadium oxide, rhenium oxide, chromium oxide, iron oxide, niobium oxide, molybdenum oxide, tungsten oxide, and potassium oxide catalysts. The fractional surface coverages given in Table 1 are calculated based on the weight percent of the specific supported metal oxide that corresponds to monolayer coverage as determined by Raman spectroscopy. The kinetic studies also employed catalysts impregnated with both vanadium oxide (0.1 to 0.2 monolayer) and a secondary metal oxide additive (0.7 to 0.9 monolayer of rhenium oxide, chromium oxide, iron oxide, niobium oxide, molybdenum oxide, tungsten oxide, or potassium oxide).

TABLE 1

Composition of Catalysts Studied

Catalyst	*V* (atoms/nm^2)	*V* (surface coverage)	*M* (atoms/nm^2)	*M* (surface coverage)
TiO_2	—	—	—	—
1% V_2O_5/TiO_2	1.3	0.17	—	—
1% Fe_2O_3/TiO_2	—	—	0.6	0.2
1% Re_2O_7/TiO_2	—	—	0.4	0.2
1% CrO_3/TiO_2	—	—	1.0	0.2
1% Nb_2O_5/TiO_2	—	—	0.8	0.1
1% MoO_3/TiO_2	—	—	0.7	0.1
1% WO_3/TiO_2	—	—	0.5	0.1
1% K_2O/TiO_2	—	—	2.4	~1
5% V_2O_5/TiO_2	6.5	0.83	—	—
5% Fe_2O_3/TiO_2	—	—	3.0	0.8
5% Re_2O_7/TiO_2	—	—	2.0	0.8
5% CrO_3/TiO_2	—	—	5.3	0.8
5% Nb_2O_5/TiO_2	—	—	4.1	0.7
5% MoO_3/TiO_2	—	—	3.3	0.7
7% WO_3/TiO_2	—	—	3.3	0.8
1% V_2O_5/5% Fe_2O_3/TiO_2	1.3	0.17	3.0	0.8
1% V_2O_5/5% Re_2O_7/TiO_2	1.3	0.17	2.0	0.8
1% V_2O_5/5% CrO_3/TiO_2	1.3	0.17	5.3	0.8
1% V_2O_5/5% Nb_2O_5/TiO_2	1.3	0.17	4.1	0.7
1% V_2O_5/5% MoO_3/TiO_2	1.3	0.17	3.3	0.7
1% V_2O_5/7% WO_3/TiO_2	1.3	0.17	3.3	0.8
1% V_2O_5/1% K_2O/TiO_2	1.3	0.17	2.4	~1

Catalysts were prepared on a TiO_2 support (Degussa P-25, 55 m^2/g), which was washed with distilled water and isopropanol (Fisher-certified ACS, 99.9% pure), dried at 120°C for 4 h, ramped at 5°C/min from 120 to 450°C, and calcined at 450°C for 2 h prior to impregnation. The V_2O_5/TiO_2 catalysts were prepared by incipient wetness impregnation. Vanadium triisopropoxide was used as the vanadium precursor. The air and moisture sensitive nature of the vanadium alkoxide precursor required the preparation of vanadia catalysts to be performed under a nitrogen environment using nonaqueous solutions. Solutions of known amounts of vanadium triisopropoxide (Alfa) and isopropanol, corresponding to incipient wetness impregnation volume and the final amount of vanadia required, were prepared in a glove box and dried at room temperature for 16 h. The impregnated samples were subsequently heated at 120°C (2 h) and 300°C (2 h) in flowing nitrogen (Linde, 99.995% pure). The final calcination was performed in oxygen at 450°C for 2 h. A 5°C/min temperature ramp was used between each stage of heating.

The other supported metal oxide catalysts were also prepared by aqueous incipient wetness impregnation under an air environment. Perrhenic acid (Aldrich, 99.99% pure), chromium (III) nitrate (Alfa, 99.999% pure), iron (III) nitrate nonahydrate (Aldrich, 99.99% pure), niobium oxalate (Aldrich, 99.999% pure), ammonium molybdate (VI) tetrahydrate (Aldrich, 99.999% pure), ammonium

metatungstate (Aldrich, 99.99% pure), and a 3% potassium hydroxide aqueous stock solution (Fisher, 99.999% pure) were used as precursors. The impregnated samples were dried at room temperature overnight and subsequently heated at 120°C (2 h), 300°C (2 h), and 450°C (2 h) in flowing oxygen. Supported vanadia catalysts with secondary metal oxide additives were similarly prepared by impregnation of a calcined 1% V_2O_5/TiO_2 catalyst with the additive precursor.

Raman Spectrometer

Raman spectra were obtained for all the catalysts in order to obtain molecular structural information about the surface metal oxide phases on the titania support. An Ar^+ laser (Spectra Physics, model 2020-50) tuned to 514.5 nm delivered 10–30 mW of power measured at the sample. The scattered radiation from the sample was directed into a Spex Triplemate spectrometer (model 1877) coupled to a Princeton Applied Research (model 1463) OMA III optical multichannel photodiode array detector. The detector was thermoelectrically cooled to −35°C to decrease the thermal noise. Twenty 30-s scans with a resolution of $<2\ cm^{-1}$ were averaged to produce the final composite spectra. Approximately 100–200 mg of the pure catalysts were made into self-supporting wafers and placed in the *in situ* Raman cell. The *in situ* Raman cell consists of a stationary holder, which has been described elsewhere (6). The *in situ* cell was heated to 300°C for 1/2 h and then cooled to room temperature in order to dehydrate the samples before the Raman spectra were obtained. The entire procedure was performed in a stream of flowing oxygen (Linde, 99.99% pure) over the catalyst sample to ensure complete oxidation of the catalysts.

Sulfur Dioxide Oxidation Reaction System

As shown in Fig. 1, kinetic studies of sulfur dioxide oxidation were performed in a heat-traced quartz reactor system with an on-line gas chromatograph (HP 5890 A) with two sulfur oxide sensitive detectors: thermal conductivity (TCD) and sulfur chemiluminescence (SCD, Sievers 355). Ultrahigh-purity helium (Linde, 99.999% pure), which has been passed through water (Alltech), hydrocarbon (Alltech), and oxygen traps (Alltech), is used as the carrier gas. Product and feed gases are sampled by a 10-port valve (Valco) constructed of a sulfur resistant material (Nitronic 50) and equipped with two 100-μL sampling loops. Two identical packed columns (6 ft. × 1/4 in. OD glass column packed with Chromosorb 107) running in parallel are installed prior to the detectors. Separation is accomplished in 5 min using an isothermal chromatograph oven temperature of 200°C. All of the GC's external lines and the injection valve are heated to at least 200°C to prevent the adsorption of sulfur oxides. Data acquisition from the detectors and control of the chromatograph's operation is handled by a desktop computer running a dedicated program (HP Chemstation V 4.0).

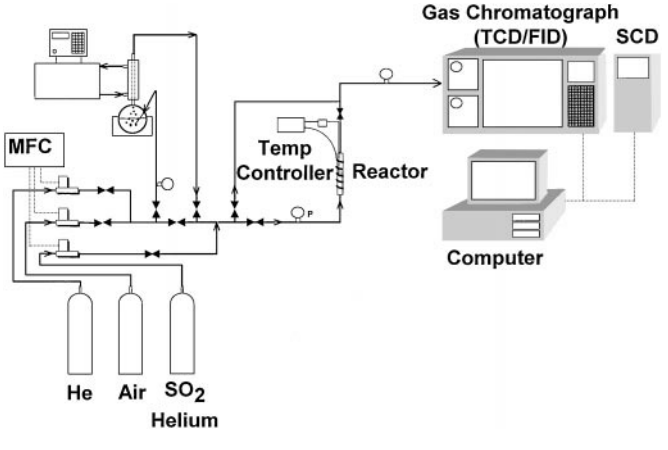

FIG. 1. Microreactor system used during kinetic studies.

TABLE 2

Standard Operating Conditions for Kinetic Studies

	Range tested	Standard condition
Reactor temperature (°C)	320 to 400	400
Gas hourly space velocity (h^{-1})	10,000 to 40,000	10,000
Feed flowrate (sccm)	160	160
Feed SO_2 partial pressure (ppm)	1000	1000
Feed O_2 partial pressure (%)	10	10
SO_2 conversion (%)	0.1 to 30	<10
Catalyst particle size range (μm)	80 to 200	80 to 200
Catalyst charge (mg)	100 to 1000	500

Reaction temperature was generally varied between 320 and 400°C. Varying the catalyst charge to the microreactor allowed space velocities to range from 10,000 to 40,000 h^{-1}, while maintaining a constant feed flowrate of 160 sccm. Sulfur dioxide and oxygen concentrations in the feed gas were maintained at 1000 ppm and 10%, respectively. The standard operating conditions for the sulfur dioxide oxidation kinetic experiments that were performed are summarized in Table 2. Assuming standard operating conditions, SO_2/He and O_2/He gas diffusivities were calculated. Effectiveness factors, based on these diffusivities, were calculated to be between 0.99 and 1.00 for the catalyst particle sizes tested, i.e., 80–200 μm, indicating that heat and mass transfer limitations were not present during these studies (7).

RESULTS

Molecular Structures of Binary Catalysts

The dehydrated Raman spectra of the low and high surface coverage titania supported metal oxide catalysts are

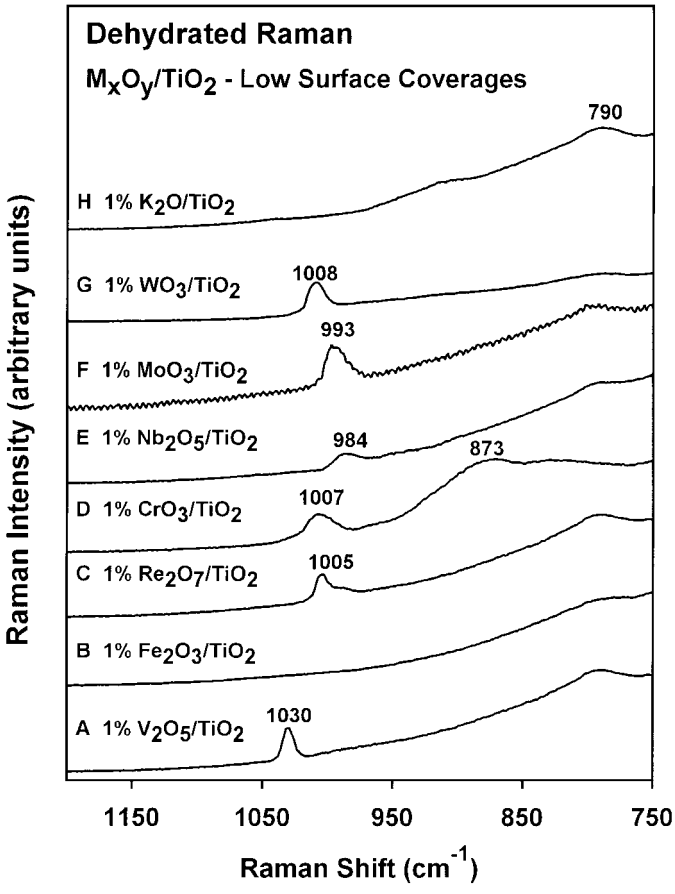

FIG. 2. Dehydrated Raman spectra of low surface coverage titania supported catalysts. (A) 1% V_2O_5/TiO_2; (B) 1% FeO_3/TiO_2; (C) 1% Re_2O_7/TiO_2; (D) 1% CrO_3/TiO_2; (E) 1% Nb_2O_5/TiO_2; (F) 1% MoO_3/TiO_2; and (G) 1% WO_3/TiO_2.

shown in Figs. 2 and 3, respectively. The weak Raman band at approximately 790 cm^{-1} is due to the TiO_2 (anatase) component of the support. The Raman bands between 980 and 1030 cm^{-1} are assigned to the terminal $M{=}O$ vibration (where $M = V$, Re, Cr, Nb, Mo, or W) of the surface metal oxide species (8). Raman bands characteristic of the bridging M–O–M bonds, 860 to 940 cm^{-1}, associated with polymerized surface species are also found in the spectra of the high surface coverage vanadium, chromium, niobium, and molybdenum oxide supported catalysts. Titania supported iron oxide catalysts do not posses Raman active vibrations in the 800 to 1200 cm^{-1} spectral region because of the absence of terminal Fe=O bonds and are overshadowed by the strong TiO_2 (anatase) bands below 800 cm^{-1}. However, surface iron oxide species on an Al_2O_3 support exhibited a broad Raman band at approximately 750 cm^{-1} (9). The other metal oxides (Re^{7+}, Cr^{6+}, Mo^{6+}, W^{6+}, V^{5+}, and Nb^{5+}) exhibit strong Raman bands in the 900 and 1000 cm^{-1} region, which are indicative of terminal $M{=}O$ bonds (8).

Raman spectroscopy is very sensitive to the appearance of microcrystalline metal oxide particles since their Raman cross sections are usually orders of magnitude greater than those of the corresponding surface metal oxide species. The major vibrations of the corresponding metal oxide microcrystals (e.g., V_2O_5, 994 cm^{-1}; α-Fe_2O_3, 410 cm^{-1}; T–Nb_2O_5, 680 cm^{-1}; α-MoO_3, 815 cm^{-1}; and WO_3, 808 cm^{-1}) usually occur at different frequencies than the strongest vibrations of the surface metal oxide species (typically ~1000 cm^{-1} due to the presence of terminal $M{=}O$ bonds) (8, 9). The absence of Raman bands characteristic of metal oxide microcrystals in Figs. 2 and 3 confirm the presence of only two-dimensional surface metal oxide overlayers on the titania support. It was not possible to rule out the existence of α-Fe_2O_3 and T-Nb_2O_5 microcrystals due to their overlap with the Raman vibrations of the TiO_2 support. Previous Raman and IR studies have shown that monolayer loadings of the titania supported catalysts correspond to 6% V_2O_5/TiO_2 (~7.9 V atoms/nm^2) (8), 6% CrO_3/TiO_2 (~6.4 Cr atoms/nm^2) (8), 7% Nb_2O_5/TiO_2 (~5.8 Nb atoms/nm^2) (8), 7% MoO_3/TiO_2 (~4.6 Mo atoms/nm^2) (8), 9% WO_3/TiO_2 (~4.2 W atoms/nm^2) (8), 6% Fe_2O_3/TiO_2 (~3.9 Fe atoms/nm^2), (8), and 1% K_2O/TiO_2 (~2.5 K atoms/nm^2)

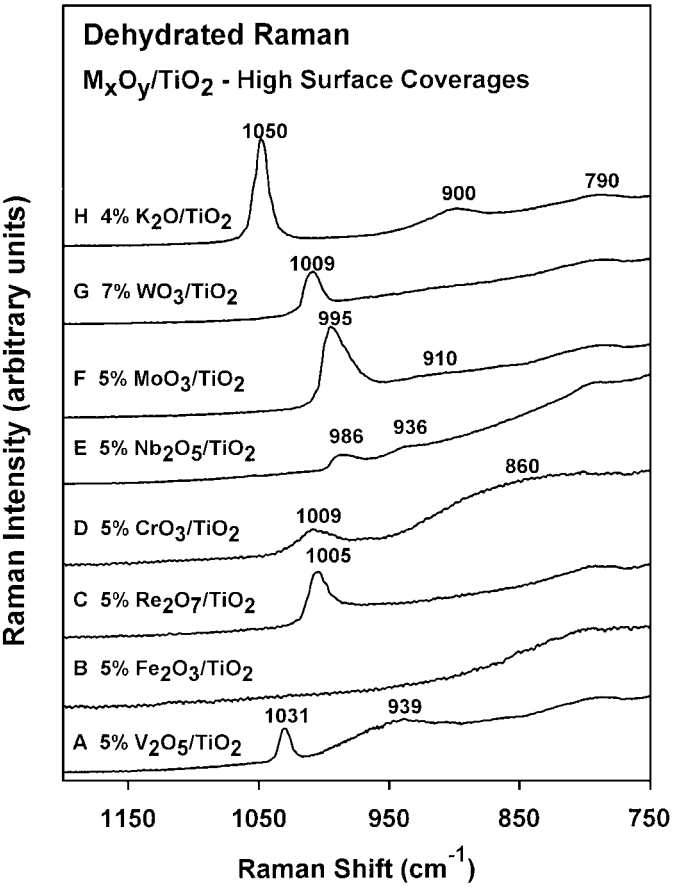

FIG. 3. Dehydrated Raman spectra of high surface coverage titania supported catalysts. (A) 5% V_2O_5/TiO_2; (B) 5% Fe_2O_3/TiO_2; (C) 5% Re_2O_7/TiO_2; (D) 5% CrO_3/TiO_2; (E) 5% Nb_2O_5/TiO_2; (F) 5% MoO_3/TiO_2; (G) 7% WO_3/TiO_2; and (H) 4% K_2O/TiO_2.

(11). However, it is not possible to create a complete monolayer of surface rhenium oxide species on the titania support due to Re_2O_7 volatilization and the highest rhenium oxide surface coverages achieved to date correspond to 6% Re_2O_7/TiO_2 (~2.4 Re atoms/nm^2) (12). Thus, the supported metal oxide catalysts employed in the present study possessed less than monolayer coverage and were essentially 100% dispersed as surface metal oxide species.

At low surface coverages (<0.2 monolayer), solid-state ^{51}V NMR (13, 14), XANES (15–17), and UV–vis DRS studies (18, 19) have shown that the dehydrated surface vanadium, chromium, rhenium, niobium, molybdenum, and tungsten oxide species supported on titania generally tend to possess fourfold coordination. The absence of strong *M*–O–*M* Raman vibrations indicate that the surface species are predominately isolated. Raman (20–25), IR (20, 24), and oxygen-18 exchange (23) experiments have suggested a mono-oxo structure for the isolated four-coordinated surface oxides of vanadium, chromium, niobium, molybdenum, and tungsten. In contrast, Raman and IR studies have suggested that the surface ReO_4 species possess three terminal Re=O bonds and one bridging Re–O–Ti bond (12). Mossbauer spectroscopy (10) has demonstrated that for low surface coverages (<0.5 Fe atoms/nm^2, corresponds to <0.13 monolayer) of iron oxide on a titania support, the dehydrated surface iron oxide species are primarily sixfold coordinated. Surface potassium oxide species preferentially titrate Lewis acid sites on the titania support to form Ti–O–K species, which increase the surface basicity (26).

At high surface coverages (> 0.6 monolayer), the coordination of the dehydrated surface metal oxide species depends on the specific metal oxide and strong Raman signals due to polymerized surface species are also usually present (surface vanadia, chromia, molybdena, tungsta, and niobia) (8). However, the surface rhenium oxide species on titania do not possess Raman vibrations due to polymerized surface species and remain isolated at all coverages. Fourfold coordination is preferred for surface rhenium oxide, chromium oxide, and vanadium oxide species, while sixfold coordination is preferred for surface molybdenum oxide, tungsten oxide and niobium oxide species. Mossbauer spectroscopy has determined that the dehydrated surface iron oxide species present on the titania support remain sixfold coordinated at surface coverages approaching monolayer coverage (10), but little information is currently available about the extent of polymerization of surface iron oxide species.

Molecular Structures of Ternary Catalysts

The dehydrated molecular structures of catalysts impregnated with both vanadium oxide (0.17 monolayer) and a secondary metal oxide additive (0.7 to 0.9 monolayer of iron oxide, rhenium oxide, chromium oxide, niobium oxide, molybdenum oxide, tungsten oxide, or potassium oxide)

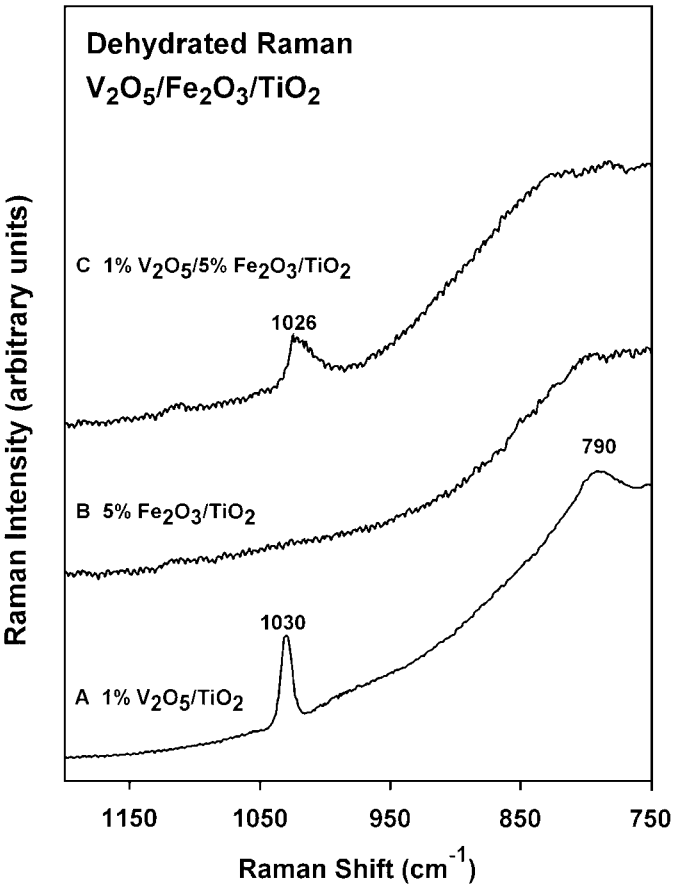

FIG. 4. Dehydrated Raman spectra of ternary and respective binary catalysts: (A) 1% V_2O_5/TiO_2; (B) 5% Fe_2O_3/TiO_2; and (C) 1% V_2O_5/5% Fe_2O_3/TiO_2.

were also investigated with Raman spectroscopy. As can be seen in Figs. 4 through 9, there appears to be only minor structural interactions between the surface vanadium oxide species and the surface iron, rhenium, chromium, niobium, molybdenum, and tungsten oxide species since the Raman band positions of the ternary catalysts are not shifted significantly relative to the respective binary catalysts. There does seem to be a slight increase in the intensity of the 880 to 930 cm^{-1} bands of the surface vanadia species, which can be attributed to an increase in the ratio of polymerized to isolated surface species caused by lateral interactions between the surface metal oxide additives and the surface vanadia species. The 986 cm^{-1} band in the Raman spectra of 5% Nb_2O_5/TiO_2 (Fig. 7b) does not appear in the spectra of 1% V_2O_5/5% Nb_2O_5/TiO_2 (Fig. 7c) due to masking by the coloration of the catalyst. Broadening of the Raman band assigned to the terminal V=O bond of the surface vanadia species occurs upon addition of iron oxide (Fig. 4), rhenium oxide (Fig. 5), and chromium oxide (Fig. 6) to the 1% V_2O_5/TiO_2 catalyst. This is due to minor lateral interactions, which increase disorder on the catalyst surface. There is no indication of metal oxide microcrystal

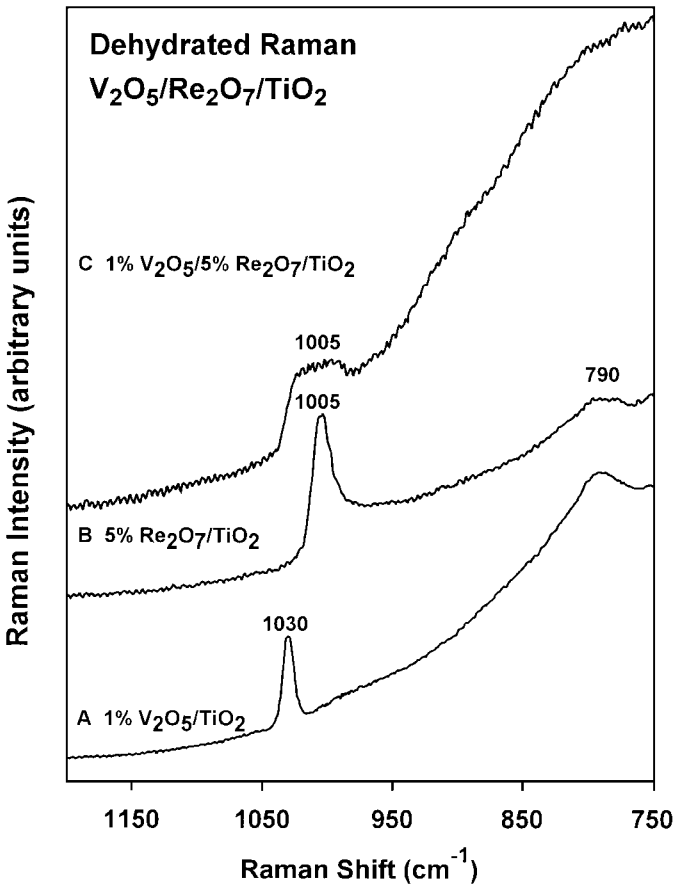

FIG. 5. Dehydrated Raman spectra of ternary and respective binary catalysts: (A) 1% V_2O_5/TiO_2; (B) 5% Re_2O_7/TiO_2; and (C) 1% V_2O_5/5% Re_2O_7/TiO_2.

formation in the spectra of the ternary catalysts, which confirms the submonolayer coverages of the ternary catalysts and 100% dispersion of the surface metal oxide species.

The addition of potassium oxide to the supported vanadia catalyst has a more pronounced effect on the surface vanadium oxide species as is evident from the Raman spectra of the 1% V_2O_5/1% K_2O/TiO_2 system (Fig. 10). The addition of approximately one monolayer of potassium oxide shifts the Raman band associated with the terminal V=O bond to 980 to 1000 cm^{-1}, which corresponds to an increase in the bond length of the V=O bond of approximately 0.02 Å (27). Previous solid state ^{51}V NMR (28) studies indicated that the surface vanadia species retains its fourfold coordination upon addition of K_2O. Furthermore, Raman dehydration studies found no evidence of crystalline vanadium–potassium oxide compound formation in the 1% V_2O_5/1% K_2O/TiO_2 sample.

Sulfur Dioxide Oxidation Activity of Binary and Ternary Catalysts

The sulfur dioxide oxidation turnover frequencies at 400°C (i.e., the number of SO_2 molecules oxidized per surface metal oxide site per second) of the binary catalysts are shown in Fig. 11 and are all within an order of magnitude ($V_2O_5/TiO_2 > Fe_2O_3/TiO_2 > Re_2O_7/TiO_2 \sim CrO_3/TiO_2 \sim Nb_2O_5/TiO_2 > MoO_3/TiO_2 \sim WO_3/TiO_2$) with the exception of K_2O/TiO_2, which is apparently inactive for sulfur dioxide oxidation under the selected reaction conditions. As metal oxide overlayer surface coverage was increased from ~0.15 to ~1.0 monolayer, the sulfur dioxide oxidation turnover frequency was approximately constant.

The sulfur dioxide conversions of the ternary supported metal oxide catalysts are shown in Table 3 along with the conversions of the corresponding binary catalysts. The reactivity studies of the binary catalysts suggest that with the exception of K_2O, all of the surface species present in the ternary catalysts (i.e., oxides of V, Fe, Re, Cr, Nb, Mo, and W) can undergo redox cycles and oxidize sulfur dioxide to sulfur trioxide to some extent. With the exception of $V_2O_5/K_2O/TiO_2$, a comparison of the activities of the ternary catalysts with the corresponding binary catalysts indicates that the vanadium oxide and the additive supported metal oxide surface redox sites are essentially acting independently without synergistic interactions, since the sum

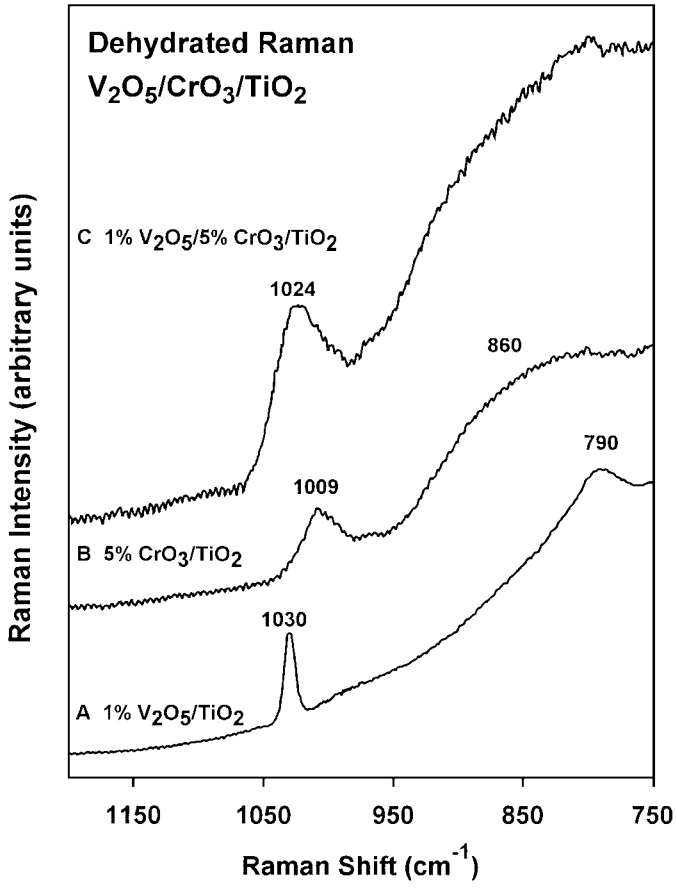

FIG. 6. Dehydrated Raman spectra of ternary and respective binary catalysts: (A) 1% V_2O_5/TiO_2; (B) 5% CrO_3/TiO_2; and (C) 1% V_2O_5/5% CrO_3/TiO_2.

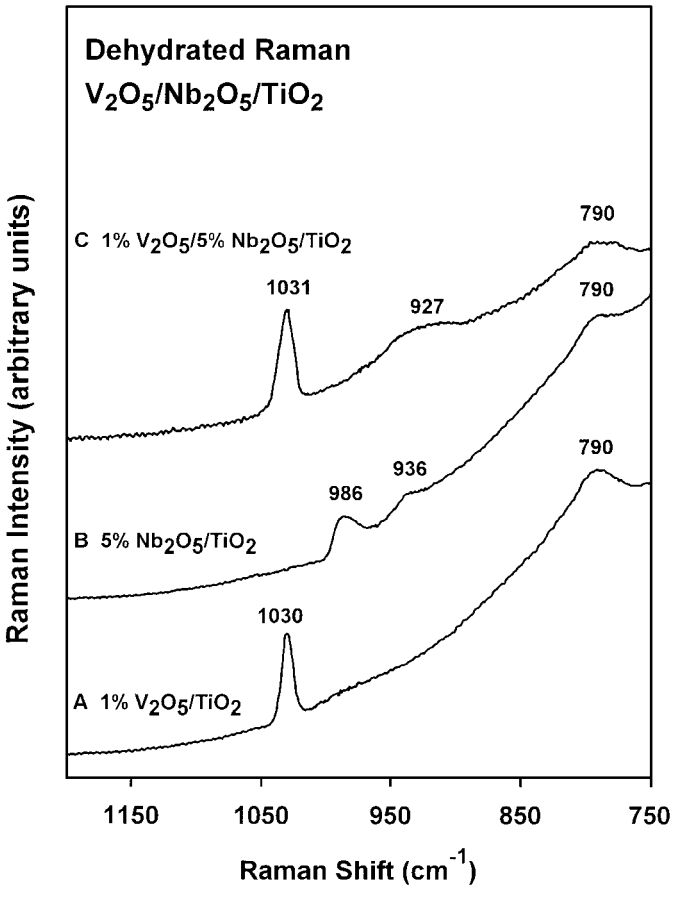

FIG. 7. Dehydrated Raman spectra of ternary and respective binary catalysts: (A) 1% V_2O_5/TiO_2; (B) 5% Nb_2O_5/TiO_2; and (C) 1% V_2O_5/5% Nb_2O_5/TiO_2.

of the activities of the individual binary catalysts may be added to yield the activity of the corresponding ternary catalyst system. The absence of synergistic interactions is expected for single-site reactions such as sulfur dioxide oxidation, whereas dual site reactions, e.g., SCR of NO_x with NH_3, will exhibit an increase in turnover frequency as surface coverage increases. The promotional effect for dual site reactions can be attributed to the increasing surface density of neighboring reaction sites as surface coverages approach monolayer. In contrast, the potassium promoted ternary catalyst deactivated the V_2O_5/TiO_2 catalyst by direct interaction of the K_2O with the surface vanadia species and reduction of its redox potential (11) caused by interaction of K^+ cations with the V–O–Ti bond (29).

DISCUSSION

As discussed above, at low surface coverages (<0.2 monolayer) the dehydrated surface vanadium, chromium, rhenium, niobium, molybdenum, and tungsten oxide species supported on titania generally tend to possess fourfold coordination and the absence of strong *M*–O–*M* Raman vibrations indicate that the surface species are predominately isolated. At high surface coverages (> 0.6 monolayer), however, the coordination of the dehydrated surface metal oxide species depends on the specific metal oxide and strong Raman signals due to polymerized surface species are also usually present (surface vanadia, chromia, molybdena, tungsta, and niobia). Fourfold coordination is preferred for surface rhenium oxide, chromium oxide, and vanadium oxide species, while sixfold coordination is preferred for surface iron oxide, molybdenum oxide, tungsten oxide, and niobium oxide species. The observation that the turnover frequency for SO_2 oxidation over all of these catalysts is approximately the same at both low and high surface coverages indicates that the mechanism of sulfur dioxide oxidation is not sensitive to the coordination of the surface metal oxide species. Furthermore, SO_2 oxidation occurs at similar rates over both isolated and polymerized surface metal oxide species, which is expected for a reaction requiring only one active site (30).

The redox properties of the titania supported metal oxide catalysts have also been probed with the partial oxidation of methanol to formaldehyde and followed a trend

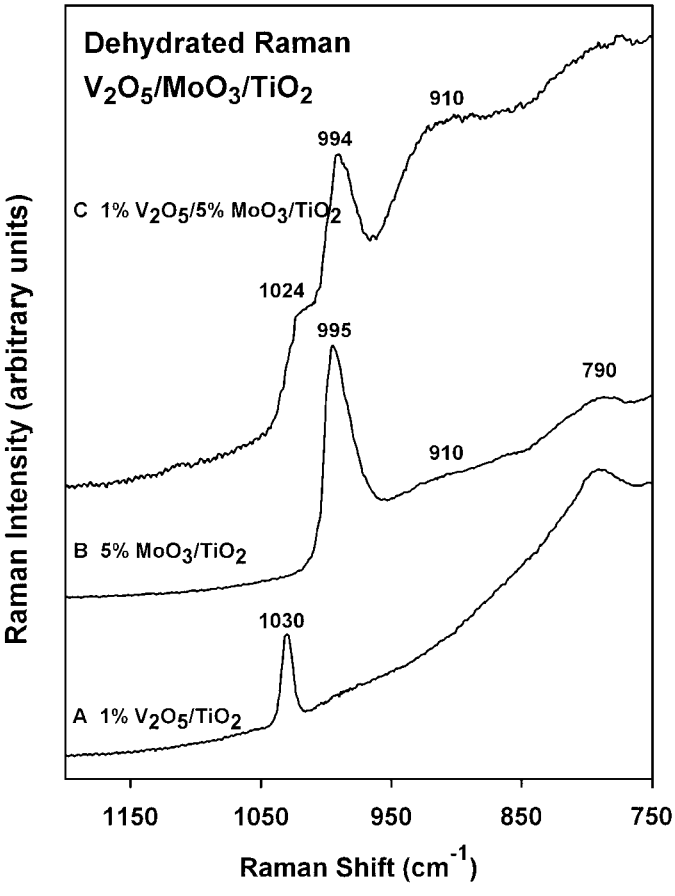

FIG. 8. Dehydrated Raman spectra of ternary and respective binary catalysts: (A) 1% V_2O_5/TiO_2; (B) 5% MoO_3/TiO_2; and (C) 1% V_2O_5/5% MoO_3/TiO_2.

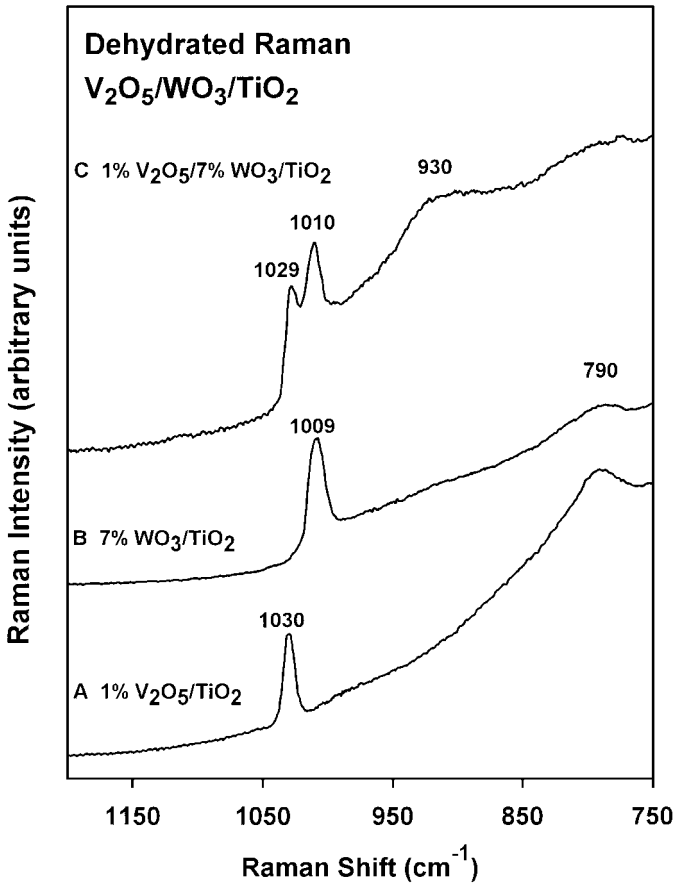

FIG. 9. Dehydrated Raman spectra of ternary and respective binary catalysts: (A)1% V_2O_5/TiO_2; (B) 7% WO_3/TiO_2; and (C) 1% V_2O_5/7% WO_3/TiO_2.

similar to that found for sulfur dioxide oxidation: $V_2O_5 \sim Re_2O_7 > CrO_3 \sim MoO_3 > Nb_2O_5 \sim WO_3 > K_2O$ (29, 31–33). The yield of selective oxidation products (e.g., formaldehyde, methyl formate, dimethoxy methane) for supported niobium oxide and tungsten oxide catalysts were approximately two orders of magnitude less than for supported vanadium oxide and rhenium oxide. Tungsten oxide was shown to increase the yield of acid products (e.g., dimethyl ether). In addition, a very similar trend was observed for methanol oxidation over niobia supported metal oxide catalysts ($V_2O_5 > CrO_3 > Re_2O_7 > MoO_3 > WO_3$) (22). These trends indicate that V_2O_5/TiO_2, Re_2O_7/TiO_2, CrO_3/TiO_2, MoO_3/TiO_2, and to a lesser degree Nb_2O_5/TiO_2 and WO_3/TiO_2 possess surface redox sites which can efficiently catalyze sulfur dioxide oxidation to sulfur trioxide. The activities of the K_2O/TiO_2 catalysts ($<5 \times 10^{-7}$ sec^{-1}) are less than that exhibited by an unpromoted TiO_2 support ($\sim 2 \times 10^{-6}$ s^{-1}) and indicate that the surface K_2O species do not undergo redox cycles at any appreciable rate under the chosen experimental conditions.

The results found in this study concerning the sulfur dioxide oxidation activities of ternary ($V_2O_5/M_xO_y/TiO_2$) catalysts are in agreement with the observation of Morikawa *et al.* (3) that V_2O_5/TiO_2 catalysts promoted by WO_3 or MoO_3 exhibit higher rates of sulfur dioxide oxidation than unpromoted catalysts, although the TOFs for WO_3/TiO_2 and MoO_3/TiO_2 are significantly lower than the TOF for V_2O_5/TiO_2. In the same study, Morikawa and coworkers found that vanadia catalysts promoted with either GeO_2 or ZnO exhibit a drastic decrease in SO_2 oxidation activity. Although no spectroscopic evidence was provided, the basic GeO_2 and ZnO molecules most likely complexed with the acidic vanadium oxide surface species and reduced their redox potentials as was seen to occur for the K_2O promoted V_2O_5/TiO_2 catalyst.

In contrast to the results found in the present study, Sazonova *et al.* (4) reported that the addition of high loadings of tungsten oxide to a V_2O_5/TiO_2 catalyst substantially suppresses sulfur dioxide oxidation activity. However, Sazonova *et al.* failed to recognize that for the loadings of surface vanadia (~3 monolayers) and tungsten oxide (~6 monolayers) species used in their study, the surface species are no longer molecularly dispersed and form WO_3 and V_2O_5 crystallites. Since no information about the

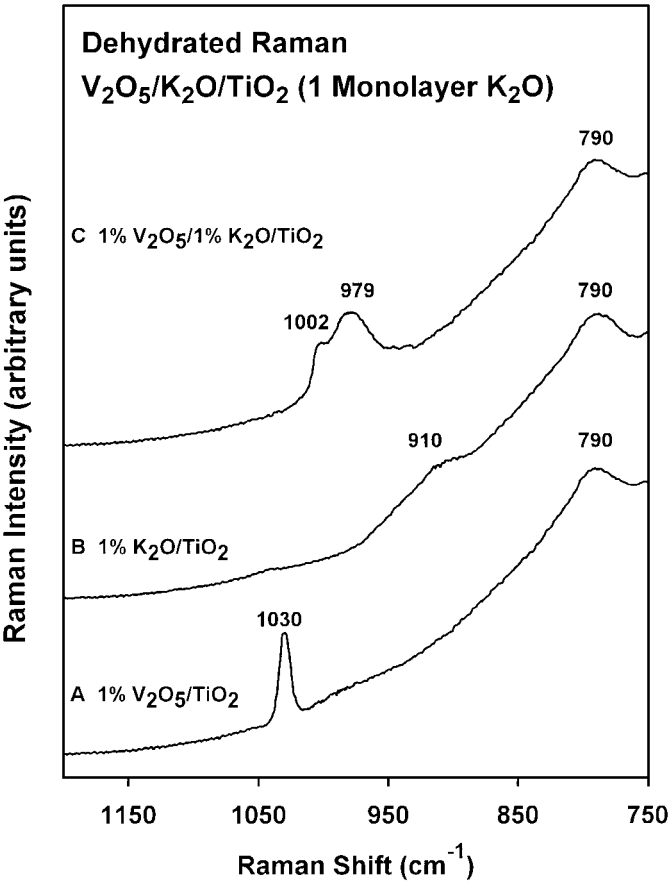

FIG. 10. Dehydrated Raman spectra of ternary and respective binary catalysts: (A) 1% V_2O_5/TiO_2; (B) 1% K_2O/TiO_2; and (C) 1% V_2O_5/1% K_2O/TiO_2.

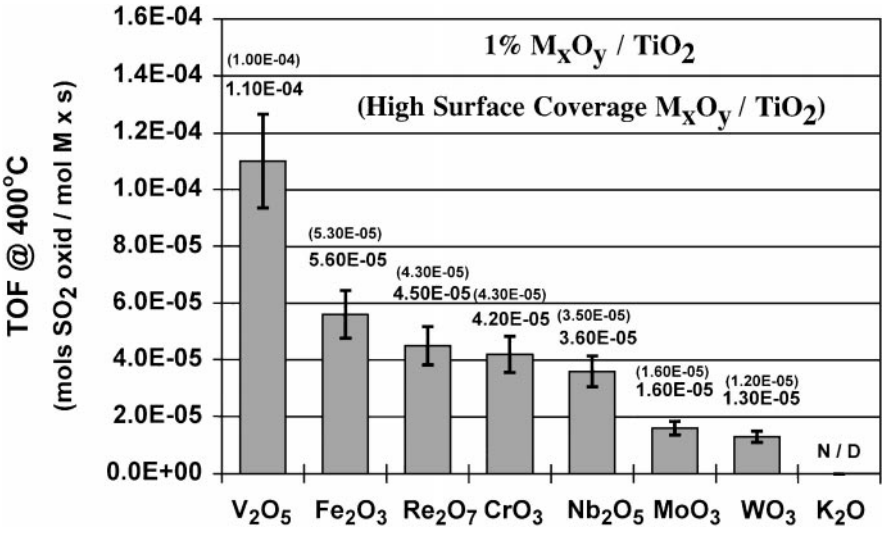

FIG. 11. SO_2 oxidation TOFs of TiO_2 supported metal oxide catalysts. Standard conditions in Table 2 followed.

structures or dispersions of the metal oxides was presented, it is not possible to clearly identify the reason for the decrease in oxidation activity; however, it is most likely due to the presence of the metal oxide crystalline phases, which are not much less active than the corresponding surface metal oxide species for redox reactions (20, 30).

TABLE 3

Conversion of Sulfur Dioxide for Binary and Ternary Catalysts

Catalyst	SO_2 conversion (%)	
	320°C	400°C
TiO_2	<0.2	0.4
1% V_2O_5/TiO_2	1.6	7.2
5% Fe_2O_3/TiO_2	3.1	15.2
1% V_2O_5/5% Fe_2O_3/TiO_2	4.5 (4.7)[a]	23.4 (22.4)[a]
1% V_2O_5/TiO_2	1.6	7.2
5% Re_2O_7/TiO_2	2.9	14.8
1% V_2O_5/5% Re_2O_7/TiO_2	4.4 (4.5)[a]	21.0 (22.0)[a]
1% V_2O_5/TiO_2	1.6	7.2
5% CrO_3/TiO_2	2.7	13.3
1% V_2O_5/5% CrO_3/TiO_2	4.0 (4.3)[a]	20.1 (20.5)[a]
1% V_2O_5/TiO_2	1.6	7.2
5% Nb_2O_5/TiO_2	2.4	11.0
1% V_2O_5/5% Nb_2O_5/TiO_2	3.6 (4.0)[a]	17.5 (18.2)[a]
1% V_2O_5/TiO_2	1.6	7.2
5% MoO_3/TiO_2	1.4	8.1
1% V_2O_5/5% MoO_3/TiO_2	2.8 (3.0)[a]	13.9 (15.3)[a]
1% V_2O_5/TiO_2	1.6	7.2
7% WO_3/TiO_2	1.7	10.1
1% V_2O_5/7% WO_3/TiO_2	3.3 (3.3)[a]	17.1 (17.3)[a]
1% V_2O_5/TiO_2	1.6	7.2
1% K_2O/TiO_2	<0.2	<0.2
1% V_2O_5/1% K_2O/TiO_2	<0.2 (1.6)[a]	<0.2 (7.2)[a]

Note. Standard operating conditions listed in Table 2 followed.

[a] Conversion calculated by the addition of the binary catalysts' conversions.

It has been proposed by Lietti *et al.* (34) that electronic interactions between neighboring surface vanadia and surface tungsten oxide sites on a titania support may lead to an increase in both SCR $DeNO_x$ and sulfur dioxide oxidation activities at temperatures below 230°C. This is based on the observation that the reactivity of a ternary (i.e., 1.4% V_2O_5/9% WO_3/TiO_2) catalyst in the SCR reaction is higher than that of the corresponding binary (i.e., 1.4% V_2O_5/TiO_2 and 9% WO_3/TiO_2) catalysts physically combined. Lietti *et al.* acknowledge that at temperatures above 230°C this synergism is due to both the increased Brønsted acidity and higher total surface coverage of the ternary catalyst relative to the binary catalysts, which allows the dual-site mechanism of the SCR reaction to proceed more efficiently. However, at temperatures below 230°C they propose that (i) the SCR rate determining step is the reoxidation of the reduced surface vanadia species and (ii) the ternary catalyst possesses superior redox properties at these temperatures. The redox properties of the ternary $V_2O_5/WO_3/TiO_2$ catalysts at 200 and 230°C have been probed by the single-site sulfur dioxide oxidation (30) and selective oxidation of methanol to formaldehyde (20) reactions, respectively. However, neither study showed an increase in redox activity for the ternary catalyst with respect to the corresponding binary catalysts. Furthermore, the turnover frequency for the SCR $DeNO_x$ reaction (10^{-3} to 10^{-2} s^{-1}) is intermediate between the turnover frequencies for sulfur dioxide oxidation (10^{-6} s^{-1}) and methanol oxidation (10^{0} s^{-1}) at 230°C over supported vanadia catalysts. Therefore, there does not appear to be any evidence for an electronic interaction between the surface vanadia and tungsten oxide species of the ternary catalyst, which allows redox reactions to proceed more efficiently.

One of the primary impediments in the development of low-temperature (e.g., 200 to 300°C) SCR catalysts is the reaction between ammonia and sulfur trioxide to form ammonium sulfates, which readily deposit on the catalyst surface at temperatures below 250°C. In order to design low-temperature SCR catalysts, it is necessary to identify catalysts that can efficiently promote the SCR reaction without significantly increasing the oxidation of sulfur dioxide. Amiridis *et al.* (5) conducted a systematic investigation of the SCR activity of several of the ternary catalysts which were also evaluated above (e.g., $V_2O_5/Fe_2O_3/TiO_2$, $V_2O_5/Nb_2O_5/TiO_2$, $V_2O_5/MoO_3/TiO_2$, and $V_2O_5/WO_3/TiO_2$). Catalysts promoted with molybdenum oxide or tungsten oxide showed the highest SCR activities in the presence of nitric oxide, ammonia, oxygen, sulfur dioxide, and water. Niobium oxide and iron oxide promoted catalysts only showed a slight increase in catalytic activity in relation to the binary V_2O_5/TiO_2 catalyst. Amiridis *et al.* concluded that the promotional effect on SCR activity induced by the surface tungsten oxide and surface molybdenum oxide additives may be due to the increased Brønsted acidity exhibited by these surface metal oxide species. These studies suggest that tungsten oxide is the most efficient additive for V_2O_5/TiO_2 catalysts at promoting the selective catalytic reduction of nitric oxide and simultaneously exhibiting low activity toward the oxidation of sulfur dioxide to sulfur trioxide.

Wachs *et al.* (35) recently found that the turnover frequency of 1% Re_2O_7/TiO_2 catalysts was approximately twice as that of a 1% V_2O_5/TiO_2 catalyst for the selective catalytic reduction of nitric oxide with ammonia (3.2×10^{-4} s^{-1} vs 1.7×10^{-4} s^{-1} at 200°C). However, the selectivity for N_2 formation was depressed for the Re_2O_7/TiO_2 catalyst relative to V_2O_5/TiO_2 (~70% vs ~100%). This observation, coupled with the present observation that the sulfur dioxide oxidation turnover frequency of Re_2O_7/TiO_2 is less than half that of V_2O_5/TiO_2, suggests that a catalyst containing low loadings (0.1 to 0.2 monolayer) of surface rhenium oxide and higher loadings (0.7 to 0.9 monolayer) of surface tungsten oxide may be an efficient low-temperature SCR catalyst.

CONCLUSIONS

A systematic investigation of the sulfur dioxide oxidation reactivity of several binary and ternary supported metal oxide catalysts was conducted. Raman spectroscopy provided information about the surface molecular structures of the two-dimensional metal oxide overlayers on the titania support and revealed that the metal oxides were essentially 100% dispersed as surface metal oxide species.

The molecular structures of catalysts impregnated with both vanadium oxide and a secondary metal oxide additive indicated that only minor structural interactions occur between the surface vanadium oxide and iron, rhenium, chromium, niobium, molybdenum, and tungsten oxide species. The addition of monolayer coverages of potassium oxide to the supported vanadia catalyst had a more pronounced effect on the surface vanadium oxide species and resulted in an increase in the bond length of the V=O bond, but there was no evidence of vanadium–potassium compound formation in the 1% V_2O_5/1% K_2O/TiO_2 sample.

The sulfur dioxide oxidation turnover frequencies of the binary catalysts were all within an order of magnitude ($V_2O_5/TiO_2 > Fe_2O_3/TiO_2 > Re_2O_7/TiO_2 \sim CrO_3/TiO_2 \sim Nb_2O_5/TiO_2 > MoO_3/TiO_2 \sim WO_3/TiO_2$) with the exception of K_2O/TiO_2, which is apparently inactive for sulfur dioxide oxidation under the specified reaction conditions. With the exception of K_2O, all of the surface species present on the ternary catalysts (i.e., oxides of V, Fe, Re, Cr, Nb, Mo, and W) can undergo redox cycles and oxidize sulfur dioxide to sulfur trioxide. The observation that the turnover frequency for SO_2 oxidation over all of these catalysts is approximately the same at both low and high surface coverages indicates that the mechanism of sulfur dioxide oxidation is not sensitive to the coordination of the surface metal oxide species. Furthermore, SO_2 oxidation occurs at similar rates over both isolated and polymerized surface metal oxide species, which is expected for a reaction requiring only one active site.

A comparison of the activities of the ternary catalysts with the corresponding binary catalysts indicates that the vanadium oxide and additive oxide surface redox sites essentially act independently without synergistic interactions, since the activities of the binary catalysts may be added to give the activity of the corresponding ternary catalyst. The absence of synergistic interactions is expected for single-site reactions such as sulfur dioxide oxidation, whereas dual site reactions, e.g., SCR of NO_x, will exhibit an increase in turnover frequency as surface coverage increases. In contrast, the potassium oxide promoted ternary catalyst deactivated the V_2O_5/TiO_2 catalyst by direct interaction of the K_2O with the surface vanadia species and the reduction of its redox potential.

ACKNOWLEDGMENTS

Financial support of National Science Foundation Grant CTS-9626893 is gratefully acknowledged. The assistance of Dr. Chuan Bao Wang and Xingtao Gao in obtaining the Raman spectra is greatly appreciated. The binary supported chromium oxide catalysts used in this study were prepared by Yang Gao.

REFERENCES

1. Cooper, C. D., and Alley, F. C., "Air Pollution Control: A Design Approach." Waveland, Prospect Heights, IL, 1994.
2. Bosch, H., and Janssen, F. J. J. G., *Catal. Today* **2**, 369 (1988).
3. Morikawa, S., Yoshida, H., Takahashi, K., and Kurita, S., *Chem. Lett.* 251 (1981).

4. Sazonova, N., Tsykoza, L., Simakov, A., Barannik, G., and Ismagilov, Z., *React. Kinet. Catal. Lett.* **52**(1), 101 (1994).
5. Amiridis, M. D., Duevel, R. V., and Wachs, I. E., Submitted for publication.
6. Vuurman, M. A., Hirt, A. M., and Wachs, I. E., *J. Phys. Chem*. **95**, 9928 (1991).
7. Dunn, J. P., Doctoral dissertation, Lehigh Univ. Bethlehem, PA, 1998.
8. Wachs, I. E., *Catal. Today* **27**, 437 (1996).
9. Vuurman, M. A., and Wachs, I. E., *J. Mol. Catal.* **77**, 29 (1992).
10. Suo, Z.-H., Kou, Y., Niu, J.-Z., Zhang, W.-Z., and Wang, H.-L., *Appl. Catal. A* **148**, 301 (1997).
11. Courcot, D., Gengembre, L., Guelton, M., Barbaux, Y., and Grzybowska, B., *J. Chem. Soc. Faraday Trans.* **90**, 895 (1994); Courcot, D., Grzybowska, B., Barbaux, Y., Rigole, M., Ponchel, A., and Guelton, M., *J. Chem. Soc. Faraday Trans.* **92**(9), 1609 (1996).
12. Vuurman, M. A., Stufkens, D. J., Oskam, A., and Wachs, I. E., *J. Mol. Catal.* **76**(1–3), 263 (1992).
13. Eckert, H., and Wachs, I. E., *Mater. Res. Soc. Symp. Proc.* **111**, 455 (1988); Eckert, H., and Wachs, I. E., *J. Phys. Chem*. **93**, 6796 (1989); Das, N., Eckert, H., Hu, H., Wachs, I. E., Walzer, J., Feher, F., *J. Phys. Chem*. **97**, 8240 (1993).
14. Le Costumer, L. R., Taouk, B., Le Meur, M., Payen, E., Guelton, M., and Grimblot, J., *J. Phys. Chem*. **92**, 1230 (1988).
15. Tanaka, T., Yamashita, H., Tsuchitania, R., Funabiki, T., and Yoshida, S., *J. Chem. Soc. Faraday Trans.* **84**(1), 2897 (1988); Yoshida, S., Tanaka, T., Nishimura, Y., and Mizutani, H., *in* "Proceedings, 9th International Congress on Catalysis, Calgary, 1988" (J. Phillips and M. Ternan, Eds.). Chem. Institute of Canada, Ottawa, 1988; Yoshida, S., Tanaka, T., Hanada, T., Hiraiwa, T., and Kanai, H., *Catal. Lett.* **12**, 277 (1992).
16. de Boer, M., van Dillen, A. J., Koningsberger, D. C., Geus, J. W., Vuurman, M. A., and Wachs, I. E., *Catal. Lett.* **11**, 227 (1991).
17. Horsley, J. A., Wachs, I. E., Brown, J. M., Via, G. H., and Hardcastle, F. D., *J. Phys. Chem*. **91**, 4014 (1987); Hardcastle, F. D., Wachs, I. E., Horsley, J. A., and Via, G. H., *J. Mol. Catal.* **46**, 15 (1988).
18. Scharf, U., Schraml-Marth, M., Wokaun, A., and Baiker, A., *J. Chem. Soc. Faraday Trans.* **87**, 3299 (1991).
19. Weckhuysen, B. M., Schoonheydt, R. A., Deo, G., Hu, H., Jehng, J. M., and Wachs, I. E., Paper presented at 13th North American Catalysis Society Meeting, Salt Lake City, Utah, June (1995); Weckhuysen, B. M., Vannijvel, I. P., and Schoonheydt, R. A., *Zeolites* **15**, 482 (1995).
20. Deo, G., Wachs, I. E., and Haber, J., *Crit. Rev. Surf. Chem*. **4**(3/4), 141 (1994); Wachs, I. E., and Weckhuysen, B. M., *Appl. Catal. A* **157**, 67 (1997).
21. Kim, D. S., Ostromecki, M., and Wachs, I. E., *J. Mol. Catal.* **106**, 93 (1996).
22. Wachs, I. E., and Jehng, J. M., Deo, G., Hu, H., and Arora, N., *Catal. Today* 199 (1996).
23. Weckhuysen, B., and Wachs, I. E., Submitted for publication.
24. Busca, G., *Mater. Chem. Phys.* **19**, 157 (1988); Davydov, A. A., *Kinet. Katal*. **34**, 951 (1993).
25. Went, G. T., Oyama, S. T., and Bell, A. T., *J. Phys. Chem*. **94**, 4240 (1990).
26. Busca, G., Forzatti, P., Lavalley, J. C., and Tronconi, E., *in* "Studies in Surface Science and Catalysis" (B. Imelik, C. Naccache, G. Courdurierm, Y. B. Taarit, and J. C. Vedrine, Eds.), Vol. 20, Catalysis by Acids and Bases. Elsevier, Amsterdam, 1985.
27. Hardcastle, F. D., and Wachs, I. E., *J. Phys. Chem*. **95**, 5031 (1991).
28. Eckert, H., Deo, G., and Wachs, unpublished results.
29. Deo, G., and Wachs, I. E., *J. Catal.* **146**, 335 (1994).
30. Dunn, J. P., Koppula, P. R., Stenger, H. G., and Wachs, I. E., *Appl. Catal. B*, in press.
31. Wachs, I. E., Deo, G., Kim, D. S., Vuurman, M. A., and Hu, H., *J. Mol. Catal.* **83**, 443 (1993).
32. Deo, D., Jehng, J. M., Kim, D. S., Wachs, I. E., Vuurman, M. A., and Andreini, A., *in* "Environmental Catalysis" (G. Centi *et al.*, Eds.), p. 207. SCI Rome, 1995.
33. Jehng, J. M., and Wachs, I. E., *Catal. Today* **8**, 37 (1990).
34. Lietti, L., Forzatti, P., and Bregani, F., *Ind. Eng. Chem. Res.* **35**, 3884 (1996).
35. Wachs, I. E., Deo, G., Andreini, A., Vuurman, M. A., and de Boer, M., *J. Catal.* **160**, 322 (1996).